Kinematic Singularities of a 3-DoF Planar Geared Robot Manipulator

S.Vahid Amirinezhad, Peter Donelan

Kinematic Singularities of a 3-DoF Planar Geared Robot Manipulator

S.Vahid Amirinezhad and Peter Donelan

Abstract By incorporating gearing into a planar 3R mechanism, one obtains a family of mechanisms in which the gear ratios play a central kinematic role. Special choices of these parameters result in interesting simplifications of the kinematic mapping. An explicit expression for the mapping can be derived using the 'matroid method' of Talpasanu *et al* [7]. We use this relatively simple mechanism to illustrate singularity analysis for geared mechanisms.

Key words: planar manipulator, kinematic singularity, geared mechanism, matroid method

1 Introduction

The use of gear pairs in a mechanism may confer a number of advantages. For example, they can enable more efficient placement of the actuators thereby reducing their mass and inertia. Epicyclic gear trains (EGTs), in which the centre of one gear wheel revolves around that of another, are the simplest form and therefore play an important role in geared mechanisms (GMs). By utilising EGTs, we can easily place actuators close to the base of a GM and rotation of inputs can be efficiently transmitted to the end-effector. Careful choice of gear ratios can also enable end-effector motion to be tailored to specific inputs.

The fundamental kinematic equation for an epicyclic gear is due to Willis [11]. Subsequent authors have introduced methods of global analysis for GMs that ensure the equations are correctly formulated for a given mechanism topology and design. Notably, Buchsbaum and Freudenstein [3] introduced combinatoric meth-

S.Vahid Amirinezhad, Peter Donelan
School of Mathematics and Statistics, Victoria University of Wellington, PO Box 600, New Zealand
e-mail: vahid.amirinezhad@msor.vuw.ac.nz, peter.donelan@vuw.ac.nz

ods to represent the topology of the mechanism. This approach was later developed by Tsai [9], Hsu and Lam [4]. In order to enhance the computational effectiveness of the method, Talpasanu *et al.* [6, 7] refined and to some extent recast the approach, introducing the 'incidence and transfer method' that uses the cycle matroid of the mechanism's directed graph. A comparison of Talpasanu's method with that of Tsai–Tokad was made in [1]. In this paper, we illustrate Talpasanu's method for a simple geared version of a planar 3R mechanism in order to determine its kinematic mapping and thereby its singularities. The goal is to develop a systematic approach to the kinematic analysis of GMs and the determination of their singularities. While the example presented is straightforward, it is intended to provide a model for extending singularity analysis of GMs to more complex cases, including those which are genuinely spatial in their kinematics and to parallel mechanisms incorporating gearing.

2 The Mechanism

A simple planar GM consists of $n+1$ links, $L_0, \ldots, L_n$, and m joints that include t revolute (turning) pairs, $T_1, \ldots, T_t$, and g gear pairs, $G_1, \ldots, G_g$, so that $m = t + g$. Note that the number of links, excluding the base L_0, is assumed equal to the number of simple pairs, *i.e.* $t = n$. In effect, the mechanism without gears contains no closed chains.

By placing three actuator joints at the base and using simple spur-gear pairs to transmit motion to the end-effector, one obtains a geared mechanism based on a simple serial planar 3R mechanism (see Figure 1). One EGT, consisting of three gear wheels and using link L_1 as carrier, transmits motion to the link L_7, while a second EGT of five gear wheels with links L_1 and L_7 as carriers transmits motion to the end-effector.

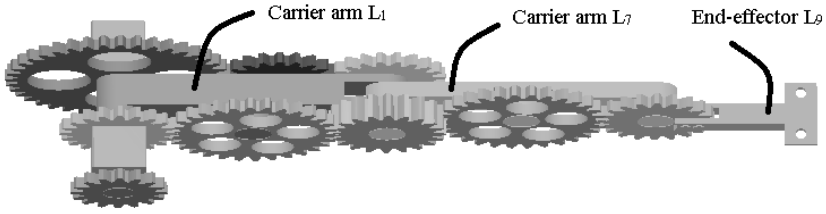

Fig. 1 3-DoF Geared Planar Manipulator

A functional schematic for the mechanism is illustrated in Figure 2. The inputs, which are attached to the base L_0, are via T_i, $i = 1, 2, 3$ while link L_9 is the output planet gear or end-effector. Note that the carrier arms L_1 and L_7 that form the first

two links in the underlying planar 3R are also gear wheels. Other links are intermediate (idler) gear wheels.

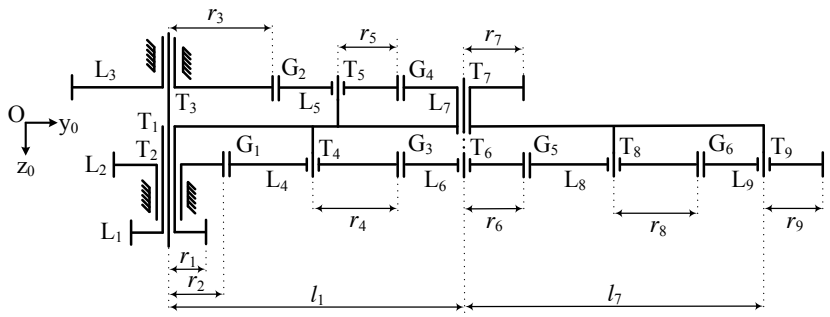

Fig. 2 Functional schematic of manipulator in Figure 1

In its directed graph (digraph) representation, Figure 3, the links (including gear wheels) are vertices $(L_0,\ldots,L_9)$ while joints are edges. Specifically, the revolute pairs $(T_1,\ldots,T_9)$ are solid edges and gear pairs $(G_1,\ldots,G_6)$ are dashed. Note that the solid edges form a spanning tree for the graph; put another way, each simple cycle contains at least one gear pair as an edge. The direction of an edge connecting vertices (links) L_i and L_j is $L_i \to L_j$ if the transmission from input to output flows from L_i to L_j.

Application of the CGK formula shows that the GM has three degrees of freedom (3 dof), noting that a gear pair has 2 dof. Alternatively, Talpasanu [6] and Tsai [9] observe that there is a relation between the degrees of freedom f of the GM, the number of links and the number of gear pairs:

$$f = n - g \tag{1}$$

again yielding $f = 3$.

3 Constraint Analysis via the Matroid Method

To perform the kinematic analysis, we apply the matroid method of Talpasanu [7] to obtain the Willis kinematic equations for all gear pairs and solve these equations to express all joint variables in terms of the input (sun) variables. This enables us to express the kinematic mapping as a product of exponentials (PoE) in terms of input variables alone and consequently to undertake the singularity analysis. It is worth noting that the Willis equations usually express the relation between angular velocities in a gear-pair/carrier cycle but since the relations between the joint variables

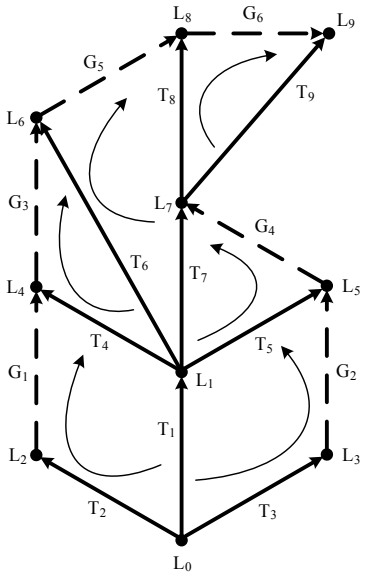

Fig. 3 Associated digraph

themselves is linear, the same equations hold between the underlying variables as between their velocities.

There are essentially three stages to the matroid or incidence–transfer method: the first stage codifies the topology of the digraph representation of the GM in matrix form. The second stage builds the specific design on to this by introducing dimensions that can then be interpreted as gear ratios. The method insures that we obtain a minimal set of linear (Willis) equations and the third stage is to solve these for the joint variables in terms of the input variables.

Associated to the digraph are two matrices. The *incidence matrix* $\mathbf{\Pi}^0$ has rows labelled by the vertices and columns by edges and its entries π^0_{ij} are -1 or 1 according as edge j leaves or enters vertex i, or else is 0. In this setting, the base L_0 is fixed and its row (containing only -1 and 0) is linearly dependent on the other rows. So, for the purpose of analysis we omit this row and arrive at the *reduced* incidence matrix $\mathbf{\Pi}$ as follows:

$$\mathbf{\Pi} = \begin{array}{c} \\ L_1 \\ L_2 \\ L_3 \\ L_4 \\ L_5 \\ L_6 \\ L_7 \\ L_8 \\ L_9 \end{array} \begin{array}{c} \begin{array}{ccccccccc|cccccc} T_1 & T_2 & T_3 & T_4 & T_5 & T_6 & T_7 & T_8 & T_9 & G_1 & G_2 & G_3 & G_4 & G_5 & G_6 \end{array} \\ \left[\begin{array}{ccccccccc|cccccc} 1 & 0 & 0 & -1 & -1 & -1 & -1 & 0 & 0 & 0 & 0 & 0 & 0 & 0 & 0 \\ 0 & 1 & 0 & 0 & 0 & 0 & 0 & 0 & 0 & -1 & 0 & 0 & 0 & 0 & 0 \\ 0 & 0 & 1 & 0 & 0 & 0 & 0 & 0 & 0 & 0 & -1 & 0 & 0 & 0 & 0 \\ 0 & 0 & 0 & 1 & 0 & 0 & 0 & 0 & 0 & 1 & 0 & -1 & 0 & 0 & 0 \\ 0 & 0 & 0 & 0 & 1 & 0 & 0 & 0 & 0 & 0 & 1 & 0 & -1 & 0 & 0 \\ 0 & 0 & 0 & 0 & 0 & 1 & 0 & 0 & 0 & 0 & 0 & 1 & 0 & -1 & 0 \\ 0 & 0 & 0 & 0 & 0 & 0 & 1 & -1 & -1 & 0 & 0 & 0 & 1 & 0 & 0 \\ 0 & 0 & 0 & 0 & 0 & 0 & 0 & 1 & 0 & 0 & 0 & 0 & 0 & 1 & -1 \\ 0 & 0 & 0 & 0 & 0 & 0 & 0 & 0 & 1 & 0 & 0 & 0 & 0 & 0 & 1 \end{array}\right] \end{array} \tag{2}$$

Further, this is partitioned as indicated into submatrices: $\mathbf{\Pi}_{n\times m} = [\mathbf{P}_{n\times t}|\hat{\mathbf{P}}_{n\times g}]$.

A *cycle basis matrix* $\mathbf{\Gamma}$ for a digraph consists of a maximally independent set of rows $G_i, i = 1,\ldots,g$, each corresponding to a cycle, whose entries $\gamma_{ij}, j = 1,\ldots,m$ are -1 or 1 according as edge j appears in that cycle directed with, or opposed to, a given vertex order for the cycle, or otherwise 0. The cycle space is in fact the nullspace of the incidence matrix so, according to Euler's formula, its dimension is $m-n$. Given the special structure of the digraph for a GM, we have $m-n = g$ and a basis for the cycle space can be indexed by the gear pairs, $G_1,\ldots,G_g$. For the given GM, with the vertex order as indicated in Figure 3 by arrows in each basis cycle, we have:

$$\mathbf{\Gamma} = \begin{array}{c} \\ G_1 \\ G_2 \\ G_3 \\ G_4 \\ G_5 \\ G_6 \end{array} \begin{array}{c} \begin{array}{ccccccccc|cccccc} T_1 & T_2 & T_3 & T_4 & T_5 & T_6 & T_7 & T_8 & T_9 & G_1 & G_2 & G_3 & G_4 & G_5 & G_6 \end{array} \\ \left[\begin{array}{ccccccccc|cccccc} -1 & 1 & 0 & -1 & 0 & 0 & 0 & 0 & 0 & 1 & 0 & 0 & 0 & 0 & 0 \\ -1 & 0 & 1 & 0 & -1 & 0 & 0 & 0 & 0 & 0 & 1 & 0 & 0 & 0 & 0 \\ 0 & 0 & 0 & 1 & 0 & -1 & 0 & 0 & 0 & 0 & 0 & 1 & 0 & 0 & 0 \\ 0 & 0 & 0 & 0 & 1 & 0 & -1 & 0 & 0 & 0 & 0 & 0 & 1 & 0 & 0 \\ 0 & 0 & 0 & 0 & 0 & 1 & -1 & -1 & 0 & 0 & 0 & 0 & 0 & 1 & 0 \\ 0 & 0 & 0 & 0 & 0 & 0 & 0 & 1 & -1 & 0 & 0 & 0 & 0 & 0 & 1 \end{array}\right] \end{array} \tag{3}$$

Again, this can be partitioned into submatrices: $\mathbf{\Gamma}_{g\times m} = [\mathbf{C}_{g\times t}|\mathbf{I}_{g\times g}]$ where the second block is the identity matrix. Note that $\mathbf{\Gamma}$ is the cycle basis matrix corresponding to the specific spanning tree for the digraph, which one can obtain by deleting the dashed lines in Figure 3. In any graph with edge set E, the collection I of subsets of E that do not include a cycle form a *matroid*, mathematical objects that capture the abstract idea of independence. Spanning trees are maximally independent while simple cycles are minimally dependent objects.

The second step is to introduce design parameters into the matrices. The constraint imposed by the cycles on the motion of the GM is captured by the *joint position matrix* $\mathbf{\Delta}$ whose entries are $\delta_{ij} = c_{ij}d_{ij}$, where c_{ij} are components of the (reduced) cycle basis matrix $\mathbf{C}$ and $d_{ij} = y_{T_j} - y_{G_i}$ where $y_{T_j}, j = 1,\ldots,t$ and $y_{G_i}, i = 1,\ldots,g$ are distances of the axes of turning joint T_j and meshing joint G_i from the base in home configuration. These distances are the radii of the various gear wheels $r_k, k = 2,\ldots,t$ so that:

$$\boldsymbol{\Delta} = \begin{array}{c} \\ G_1 \\ G_2 \\ G_3 \\ G_4 \\ G_5 \\ G_6 \end{array} \begin{array}{c} \begin{array}{ccccccccc} T_1 & T_2 & T_3 & T_4 & T_5 & T_6 & T_7 & T_8 & T_9 \end{array} \\ \begin{bmatrix} r_2 & -r_2 & 0 & -r_4 & 0 & 0 & 0 & 0 & 0 \\ r_3 & 0 & -r_3 & 0 & -r_5 & 0 & 0 & 0 & 0 \\ 0 & 0 & 0 & -r_4 & 0 & -r_6 & 0 & 0 & 0 \\ 0 & 0 & 0 & 0 & -r_5 & 0 & -r_7 & 0 & 0 \\ 0 & 0 & 0 & 0 & 0 & -r_6 & r_6 & -r_8 & 0 \\ 0 & 0 & 0 & 0 & 0 & 0 & 0 & -r_8 & -r_9 \end{bmatrix} \end{array} \tag{4}$$

For an oriented gear pair $G_i, i = 1,\ldots,g$ connecting link (gear wheel) L_p to L_q, denote the corresponding gear ratio $\rho_i = -r_p/r_q$. The rows of the matrix represent equations that hold between the joint variables at each revolute pair (or equivalently their angular velocities) so that each row can be independently scaled by one of the radii to realise the *gear ratio matrix*:

$$\boldsymbol{\Lambda} = \begin{array}{c} \\ G_1 \\ G_2 \\ G_3 \\ G_4 \\ G_5 \\ G_6 \end{array} \begin{array}{c} \begin{array}{ccccccccc} T_1 & T_2 & T_3 & T_4 & T_5 & T_6 & T_7 & T_8 & T_9 \end{array} \\ \begin{bmatrix} \rho_1 & -\rho_1 & 0 & -1 & 0 & 0 & 0 & 0 & 0 \\ \rho_2 & 0 & -\rho_2 & 0 & -1 & 0 & 0 & 0 & 0 \\ 0 & 0 & 0 & -\rho_3 & 0 & -1 & 0 & 0 & 0 \\ 0 & 0 & 0 & 0 & -\rho_4 & 0 & -1 & 0 & 0 \\ 0 & 0 & 0 & 0 & 0 & -\rho_5 & \rho_5 & -1 & 0 \\ 0 & 0 & 0 & 0 & 0 & 0 & 0 & -\rho_6 & -1 \end{bmatrix} \end{array} \tag{5}$$

To arrive finally at a complete set of Willis equations for the GM, it is necessary to incorporate the component $\mathbf{P}$ of the reduced incidence matrix that provides the connection between the angles of rotation θ_i for each link L_i and the joint variables ϕ_j at each revolute pair T_j, $i, j = 1,\ldots,n$ ($= t$ as noted in Section 2). Specifically, set:

$$\boldsymbol{\Sigma}_{g\times t} = \boldsymbol{\Lambda}_{g\times t}.\mathbf{P}^T_{t\times t}, \tag{6}$$

then the Willis equations have the matrix form:

$$\boldsymbol{\Sigma}.\boldsymbol{\theta} = \mathbf{0} \tag{7}$$

where $\boldsymbol{\theta}$ is the vector of link rotations.

We can partition $\boldsymbol{\theta}$ between *input* variables and *passive* variables. Following Eq. (1), there are three input variables and six passive variables. Explicitly:

$$\boldsymbol{\theta} = \left[\boldsymbol{\theta}_f \mid \boldsymbol{\theta}_g\right]^T = \left[\theta_1\ \theta_2\ \theta_3 \mid \theta_4\ \theta_5\ \theta_6\ \theta_7\ \theta_8\ \theta_9\right]^T \tag{8}$$

Partitioning $\boldsymbol{\Sigma}$ in a similar way, and expanding the product gives:

$$\boldsymbol{\Sigma} = \left[\boldsymbol{Z}_f \mid \boldsymbol{Z}_g\right] = \begin{array}{c} \\ G_1 \\ G_2 \\ G_3 \\ G_4 \\ G_5 \\ G_6 \end{array} \begin{array}{c} \begin{array}{ccc|ccccccc} L_1 & L_2 & L_3 & & L_4 & L_5 & L_6 & L_7 & L_8 & L_9 \end{array} \\ \left[\begin{array}{ccc|ccccccc} \rho_1+1 & -\rho_1 & 0 & & -1 & 0 & 0 & 0 & 0 & 0 \\ \rho_2+1 & 0 & -\rho_2 & & 0 & -1 & 0 & 0 & 0 & 0 \\ \rho_3+1 & 0 & 0 & & -\rho_3 & 0 & -1 & 0 & 0 & 0 \\ \rho_4+1 & 0 & 0 & & 0 & -\rho_4 & 0 & -1 & 0 & 0 \\ 0 & 0 & 0 & & 0 & 0 & -\rho_5 & \rho_5+1 & -1 & 0 \\ 0 & 0 & 0 & & 0 & 0 & 0 & \rho_6+1 & -\rho_6 & -1 \end{array}\right] \end{array} \tag{9}$$

Now, we can rewrite Eq. (7) in the form of $[\boldsymbol{Z}_f \mid \boldsymbol{Z}_g].[\boldsymbol{\theta}_f \mid \boldsymbol{\theta}_g]^T = \mathbf{0}$. from which it follows that, provided $\boldsymbol{Z}_g$ is non-singular which is easily verified in this case:

$$[\boldsymbol{\theta}_g] = -[\boldsymbol{Z}_g]^{-1}.[\boldsymbol{Z}_f].[\boldsymbol{\theta}_f] \tag{10}$$

Solving Eq. (10), gives passive variables in terms of input variables as follows:

$$\begin{bmatrix}\theta_4\\ \theta_5\\ \theta_6\\ \theta_7\\ \theta_8\\ \theta_9\end{bmatrix} = \begin{bmatrix} \rho_1+1 & -\rho_1 & 0 \\ \rho_2+1 & 0 & -\rho_2 \\ 1-\rho_1\rho_3 & \rho_1\rho_3 & 0 \\ 1-\rho_2\rho_4 & 0 & \rho_2\rho_4 \\ \rho_1\rho_3\rho_5-\rho_2\rho_4(1+\rho_5)+1 & -\rho_1\rho_3\rho_5 & \rho_2\rho_4(1+\rho_5) \\ -\rho_1\rho_3\rho_5\rho_6+\rho_2\rho_4(\rho_5\rho_6-1)+1 & \rho_1\rho_3\rho_5\rho_6 & -\rho_2\rho_4(\rho_5\rho_6-1) \end{bmatrix} . \begin{bmatrix}\theta_1\\ \theta_2\\ \theta_3\end{bmatrix} \tag{11}$$

4 Kinematic and Singularity Analysis

The forward kinematic map of the mechanism can be written in terms of the revolute pair rotations as a PoE in the relevant Euclidean group (see Murray *et al* [5]). In this case as the mechanism is planar, the group is $SE(2)$. The form of PoE derives from the corresponding *open-loop chain* (see Tsai [10]) as follows:

$$\boldsymbol{T}(\boldsymbol{\phi}) = e^{\boldsymbol{X}_1\phi_1} e^{\boldsymbol{X}_7\phi_7} e^{\boldsymbol{X}_9\phi_9} \boldsymbol{T}(\boldsymbol{0}) \tag{12}$$

where $\boldsymbol{T}(\boldsymbol{0})$ is the transformation between base and end-effector frames at the rest position $\boldsymbol{\phi} = \boldsymbol{0}$ and $\boldsymbol{X}_i$ denote the infinitesimal rotations of revolute joints T_i, $i = 1,7,9$ about their centres of rotation. Explicitly, we can use homogeneous representations as follows:

$$\boldsymbol{X}_i = \begin{bmatrix} 0 & -1 & 0 \\ 1 & 0 & -\xi_i \\ 0 & 0 & 0 \end{bmatrix} \tag{13}$$

where (with respect to appropriate choices of body coordinates) $\xi_1 = 0$, $\xi_7 = l_1$, $\xi_9 = l_1 + l_7$ with $l_1 = r_2 + 2r_4 + r_6 = r_3 + 2r_5 + r_7$ and $l_7 = r_6 + 2r_8 + r_9$ the lengths of the carrier arms L_1 and L_7 (see Figure 2); and:

$$\boldsymbol{T}(\boldsymbol{0}) = \begin{bmatrix} 1 & 0 & l_1+l_7 \\ 0 & 1 & 0 \\ 0 & 0 & 1 \end{bmatrix} \tag{14}$$

Then the homogeneous form of the forward kinematic map is

$$\boldsymbol{T}(\boldsymbol{\phi}) = \begin{bmatrix} \cos(\phi_1+\phi_7+\phi_9) & -\sin(\phi_1+\phi_7+\phi_9) & l_1\cos\phi_1 + l_7\cos(\phi_1+\phi_7) \\ \sin(\phi_1+\phi_7+\phi_9) & \cos(\phi_1+\phi_7+\phi_9) & l_1\sin\phi_1 + l_7\sin(\phi_1+\phi_7) \\ 0 & 0 & 1 \end{bmatrix} \tag{15}$$

This can be more simply expressed in terms of link rotation variables using $\theta_1 = \phi_1$, $\theta_7 = \phi_1 + \phi_7$, and $\theta_9 = \phi_1 + \phi_7 + \phi_9$. Moreover, for purposes of singularity analysis it is preferable to work with a local representation of the kinematic mapping $\mathbf{T}$. Simply using the angle θ_9 to parametrise the rotation matrix that constitutes the top left 2×2 block of the homogeneous transformation, the local representation is:

$$(\theta_1, \theta_7, \theta_9) \mapsto \begin{bmatrix} \theta_9 \\ l_1 \cos\theta_1 + l_7 \cos\theta_7 \\ l_1 \sin\theta_1 + l_7 \sin\theta_7 \end{bmatrix} \tag{16}$$

In this form, we have simply made use of the passive variables that describe the kinematics of the underlying 3R mechanism. These can now be expressed using Eq. (11) in terms of the input variables. Hence, the kinematic mapping for the GM can be expressed as a function $\mathscr{F} : \mathbb{R}^3 \to \mathbb{R}^3$, where:

$$\mathscr{F}(\theta_1, \theta_2, \theta_3) = \begin{bmatrix} \beta_1\theta_1 + \beta_2\theta_2 + \beta_3\theta_3 \\ l_1 \cos\theta_1 + l_7 \cos(\alpha_1\theta_1 + \alpha_3\theta_3) \\ l_1 \sin\theta_1 + l_7 \sin(\alpha_1\theta_1 + \alpha_3\theta_3) \end{bmatrix} \tag{17}$$

and $\alpha_1 = 1 - \rho_2\rho_4$, $\alpha_3 = \rho_2\rho_4$, $\beta_1 = -\rho_1\rho_3\rho_5\rho_6 + \rho_2\rho_4(\rho_5\rho_6 - 1) + 1$, $\beta_2 = \rho_1\rho_3\rho_5\rho_6$, and $\beta_3 = -\rho_2\rho_4(\rho_5\rho_6 - 1)$. It is worth noting that by judicious choice of gear ratios the rotation of the end-effector can be made independent of one or more input variables. For example, setting $\rho_1\rho_3 = \rho_5\rho_6 = 1$ (equivalently $r_2 = r_6 = r_9$) ensures the rotation is independent of θ_1, θ_3 and is directly equal to θ_2. This is nicely illustrated by Thang [8].

Finally, to find singularities we need to investigate the *Jacobian* of the kinematic mapping $\mathscr{F}$. From Equation (17) we obtain:

$$\mathscr{J} = \begin{bmatrix} \beta_1 & \beta_2 & \beta_3 \\ -l_1 \sin\theta_1 - \alpha_1 l_7 \sin(\alpha_1\theta_1 + \alpha_3\theta_3) & 0 & -\alpha_3 l_7 \sin(\alpha_1\theta_1 + \alpha_3\theta_3) \\ l_1 \cos\theta_1 - \alpha_1 l_7 \cos(\alpha_1\theta_1 + \alpha_3\theta_3) & 0 & \alpha_3 l_7 \cos(\alpha_1\theta_1 + \alpha_3\theta_3) \end{bmatrix} \tag{18}$$

For a singularity, we require:

$$\det(\mathscr{J}) = \alpha_3\beta_2 l_1 l_7 \sin(\theta_1 - \alpha_1\theta_1 - \alpha_3\theta_3) = 0. \tag{19}$$

The design parameters $\alpha_3, \beta_2, l_1, l_7$ are assumed non-zero so the GM is singular if and only if $\sin(\theta_1 - \alpha_1\theta_1 - \alpha_3\theta_3) = 0$ and hence:

$$\theta_1 - \theta_3 = \frac{n\pi}{\rho_2\rho_4}, \quad \text{for any integer } n.$$

Thus, the singular configurations of mechanism in Figure 1 are strictly contingent on the difference between input variables θ_1 and θ_3. It can be concluded that increasing the product of gear ratios $\rho_2\rho_4$ connecting gear wheels L_3 and L_7 can cause more singular points in the joint space, while keeping it close to zero will reduce singularities. It must be noticed that having $\rho_2\rho_4 \ll 1$ may have dynamic consequences. The

images of the singularity set in the workspace of course correspond to the expected singular configurations in which carrier arms L_1 and L_7 are collinear.

5 Conclusion

We have illustrated the constraint analysis of a geared mechanism involving two epicyclic gear trains, using the matroid method of Talpasanu. This, in turn, leads to an explicit determination of its passive variables in terms of input variables and thereby to a representation of the kinematic mapping in those variables. Determination of the the singularity set, not only in terms of specific geometric configurations in the workspace—collinearity of the carrier arms—but also in the input space, is a straightforward consequence. This demonstrates the dependency on gear ratios as design parameters for the GM.

References

1. Amirinezhad, S.V., Uyguroğlu, M.K.: Kinematic analysis of geared robotic mechanism using matroid and T–T graph methods. Mechanism and Machine Theory **88**, 16–30 (2015).
2. @bookhunt1978kinematic, title=Kinematic geometry of mechanisms, author=Hunt, Kenneth Henderson, year=1978, publisher=Clarendon Press Oxford
3. Buchsbaum, F. and Freudenstein, F.: Synthesis of kinematic structure of geared kinematic chains and other mechanisms. J. Mechanisms **5**, 357–392 (1970).
4. Hsu, C.H. and Lam, K.T.: A new graph representation for the automatic kinematic analysis of planetary spur-gear trains. J. Mech. Design **114**, 196–200 (1992).
5. Murray, R. M. and Sastry, S. S. and Zexiang, L.: A Mathematical Introduction to Robotic Manipulation. CRC Press, Inc., Boca Raton, FL (1994).
6. Talpasanu, I.: Kinematics and Dynamics of Mechanical Systems Based on Graph-Matroid Theory. Ph.D. Thesis, University of Texas at Arlington (2004).
7. Talpasanu, I., Yih, T.C., Simionescu, P.: Application of matroid method in kinematic analysis of parallel axes epicyclic gear trains. J. Mech. Design **128**, 1307–1314 (2006).
8. Thang, N.D.: Planar manipulator 3. https://www.youtube.com/watch?v=trtH7Id7HSA, (2015). Accessed 15 January 2016.
9. Tsai, L.W.: The kinematics of spatial robotic bevel-gear trains. IEEE J. Rob. Autom. **4**(2), 150–156 (1988).
10. Tsai, L.W.: Robot Analysis: the Mechanics of serial and parallel manipulators. John Wiley & Sons, New York (1999).
11. Willis, R.: Principles of Mechanism. Longmans, Green and Co., London (1870).